Journal of Histochemistry & Cytochemistry 2020 Vol. 68(7) 473–489

DOI: 10.1369/0022155420935403
journals.sagepub.com/home/jhc
SAGE

Journal of Histochemistry & Cytochemistry

A Sample Preparation Protocol for High Throughput Immunofluorescence of Suspension Cells on an Adherent Surface

Anna Bäckström, Laura Kugel, Christian Gnann, Hao Xu, Joseph E. Aslan, Emma Lundberg, and Charlotte Stadler

Department of Protein Science, Royal Institute of Technology, Stockholm, Sweden (AB, LK, CG, HX, EL, CS) and Knight Cardiovascular Institute, Oregon Health & Science University, Portland, Oregon (JEA)

Summary

Imaging is a powerful approach for studying protein expression and has the advantage over other methodologies in providing spatial information in situ at single cell level. Using immunofluorescence and confocal microscopy, detailed information of subcellular distribution of proteins can be obtained. While adherent cells of different tissue origin are relatively easy to prepare for imaging applications, non-adherent cells from hematopoietic origin, present a challenge due to their poor attachment to surfaces and subsequent loss of a substantial fraction of the cells. Still, these cell types represent an important part of the human proteome and express genes that are not expressed in adherent cell types. In the era of cell mapping efforts, overcoming the challenge with suspension cells for imaging applications would enable systematic profiling of hematopoietic cells. In this work, we successfully established an immunofluorescence protocol for preparation of suspension cell lines, peripheral blood mononucleated cells (PBMC) and human platelets on an adherent surface. The protocol is based on a multi-well plate format with automated sample preparation, allowing for robust high throughput imaging applications. In combination with confocal microscopy, the protocol enables systematic exploration of protein localization to all major subcellular structures. (J Histochem Cytochem 68: 473–489, 2020)

Keywords

immunofluorescence, Human Protein Atlas, suspension cells, automated sample preparation, subcellular profiling, organelle, confocal microscopy, PBMC, platelets

Introduction

Immunofluorescence (IF) is an application widely used to study subcellular localization of proteins to gain knowledge of protein function and it's interaction partners. Over the past 15 years, our group has contributed to establish the Human Protein Atlas (HPA) database, where immunohistochemistry and IF has been applied to systematically explore protein expression in 44 different tissue types and subcellular protein localization in selected cell lines.[1–3] The current version of the protein atlas database contains tissue profiles of nearly 20,000 proteins and subcellular localization for over 12,000 proteins. The ultimate goal of this initiative is to generate a complete map of the human proteome at both tissue and subcellular level. While most proteins are expressed and successfully stained in one or several of the 44 tissue types, the proteome-wide detection of proteins in cell lines for subcellular profiling remains a challenge. Studies using mass spectrometry show that most cell lines

Received for publication October 10, 2019; accepted May 28, 2020.

Corresponding Author:
Charlotte Stadler, Department of Protein Science, Royal Institute of Technology, Tomtebodavägen 23 A, SE-17165, Solna, Sweden.
E-mail: charlotte.stadler@scilifelab.se

Table 1. List of Coating Materials and Concentrations Used for Optimization of Cell Adherence.

Coating	FN	PLO	PLL	LN	Matrigel
Concentration (µg/ml)	12.5	12.5, 50,100	12.5, 50,100	12.5, 25,50	Dilution factor 1:30

Abbreviations: FN, fibronectin; PLO, poly-L-ornithine; PLL, poly-L-lysine; LN, laminin

express between 10 and 12,000 genes.[4,5] Within the HPA, the transcriptome of a large number of cell lines (n=64) has been analyzed using RNA sequencing[6] and the cell line panel has gradually increased to detect more of the protein coding genes.[7] Interestingly, over 4000 genes show the highest expression in any of the 16 cell lines from hematopoietic origin. Furthermore, approximately 700 of those genes are uniquely expressed within hematopoietic cell lines, making these cell lines highly valuable from a cell mapping perspective. However, most of these cell lines are not ideally suited for imaging, since they normally grow in suspension and do not readily attach to substrates in a manner needed for imaging.

Several coatings have been developed with the aim to better attach the cells to the surface.[8,9] Most coatings used today are a variety of biological materials including extracellular matrix (ECM) proteins such as collagen, laminin (LN), and fibronectin (FN). Furthermore, basic synthetic polymers, like poly-D-lysine (PDL) and poly-ornithine are also popular coatings. Some protocols and equipment have been developed to mechanically attach cells to surfaces.[10,11] However, even if suspension cells initially sediment and manage to attach to the plates or glass slides, the shear stress and flow from pipetting during the sample preparation can be sufficient to detach cells from the surface. A typical IF protocol consists of multiple steps including fixation, permeabilization, and primary and secondary antibody incubation along with several washing steps. In many cases, the sample preparation protocol itself cannot be compromised to achieve high-quality images in the end. To minimize the pipetting of the cells on the slides, some IF protocols are designed to perform most steps in solution ending with a gentle centrifugation step to sediment the cells to the imaging slide.[12] However, this is not ideal as the attachment of already fixed cells to a surface is more challenging as cells are stiffer and less flexible. Second, the benefit from observing interactions between cells is lost using this approach.

Although these efforts have resulted in better prerequisites for imaging of suspension cells, protocols for systematic high throughput and high-quality imaging of suspension cells are still lacking. Here, we present an automated IF protocol for suspension cell lines and peripheral blood cells (i.e., peripheral blood mononuclear cells [PBMC] and platelets), suitable for systematic protein profiling at high throughput.

Materials and Methods

Cell Cultivation and Coatings

For testing of different coating substrates, the T-cell derived Jurkat cell line (ACC 282, DSMZ Leibniz, Germany) was used. For testing and optimization of the automated sample preparations the following additional cell lines were included: an acute monocytic leukemia cell line THP1 (ACC-16), an erythroleukemia cell line HEL (ACC-11), a chronic myeloid leukemia cell line K-562 (ACC-10), and a B cell precursor leukemia cell line REH (ACC-22) all from DSMZ, Leibniz, Germany. The adherent osteosarcoma cell line U-2 OS (HTB-96, ATCC Wesel, Germany) was used as a reference for comparison of attachment. All cell lines were cultivated following recommendations from the providers and incubated at 37C and 5.2% CO_2. For IF 96-well glass bottom plates (Greiner Sensoplate 655891, BioNordica, Stockholm, Sweden) were coated with either FN (VWR, 734-0101), poly-L-ornithine (PLO), (A-004-M), poly-L-lysine (PLL) (P8920), and LN (L2020, all from Sigma-Aldrich, Stockholm, Sweden) at different concentrations as shown in Table 1. For FN only one concentration was tested, being the same as used routinely for our work with a panel of >20 different adherent cell lines.[1,13]

The plates were either incubated with the respective FN or LN coating solution for 1 hr at room temperature (coating solution was removed afterwards) or incubated with PLO or PLL coating solution for 5 min at room temperature followed by a washing step with 1x phosphate buffered saline (1x PBS; 137 mM NaCl, 2.7 mM KCl, 10 mM Na_2HPO_4, and 1.8 mM KH_2PO_4). Also Matrigel (catalog #324230, Corning) was tested according to the manufacturer's guidelines, by diluting it 1:30 in cell media at 4C. A total of 100 µL of diluted solution were then added to each well in the 96-well plate and incubated for 1.5 hr at room temperature or at 4C overnight before cell seeding.

Prior to this study, seeding numbers per well has been tested and optimized over the years for a broad range of cell lines used for imaging in the HPA, to reach ≈ 80% cell confluence upon fixation (data not published). Based on this experience, the following

numbers of cells were seeded per well throughout the study: 75,000 Jurkat cells; 25,000 THP1 cells; 12,000 HEL cells; 75,000 K-562 cells; 150,000 REH cells; and 8000 U-2 OS cells. For PBMC preparations between 75,000 and 110,000 cells per well were seeded directly after isolation depending on total number of isolated cells. All cells were manually seeded using a multi well pipette, carefully pipetting the cell suspension to homogenize it prior to adding cells to each column of the plates. This has shown to give reproducible cell densities within and across plates, based on the imaging done for the systematic mapping of proteins within the HPA. All cell lines and PBMC were incubated for 24 hr from seeding to fixation.

PBMC and Platelet Isolation and Seeding

PBMCs were isolated from freshly drawn blood using the BD Vacutainer CPT Mononuclear Cell Preparation Tube (CPT) (BD Biosciences, Franklin Lakes, NJ, 362761) with Ficoll-Paque as a density medium and sodium citrate as anticoagulant according to product manual guidelines.

Briefly, the CPT was filled with 7 to 8 ml of fresh blood and immediately centrifuged for 20 min at 1500 RCF. Afterwards, approximately half of the plasma layer was aspirated and the cell layer with mononuclear cells and platelets was collected in a new 15 ml centrifugation tube. The tube was then filled up to 15 ml with 1x PBS and the cells were mixed by inverting the tube five times followed by a centrifugation step for 15 min at 300 RCF. The supernatant was aspirated and the cells were resuspended in 1 ml 1x PBS by gently vortexing. The tube was then filled up to 10 ml with 1x PBS, the cells were mixed cells and centrifuged for 10 min at 300 RCF with brake on. Afterwards the cells were resuspended in 1 ml 1x PBS by gentle vortexing. To remove remaining red blood cells the eBioscience 10 X red blood cell (RBC) Lysis Buffer (Thermo Fisher Scientific, Waltham, MA, 00-4300-54) was diluted 1:10 in MilliQ water and 10 ml were added to the resuspended cells. The cells were incubated for 15 min at room temperature followed by a centrifugation step for 5 min at 300 RCF. The cells were then resuspended in PBMCs media (RPMI 1640 supplemented with 10% fetal bovine serum [FBS], 1% sodium-pyruvate, 1% penicillin-streptomycin, and 1% L-glutamine) and counted prior to seeding into the 96-well plates for IF.

Platelets were isolated and prepared as previously described.[14] Briefly, human venous blood was drawn into sodium citrate from healthy adult volunteers in accordance with an Oregon Health & Science University Institutional Review Board (IRB)-approved protocol. Platelet-rich plasma (PRP) was prepared by centrifugation of anticoagulated blood at 200 RCF for 10 min. Platelets were further purified from PRP by centrifugation at 1000 RCF in the presence of prostacyclin (PGI_2). Following wash with HEPES/Tyrode buffer (129 mM NaCl, 0.34 mM Na_2HPO_4, 2.9 mM KCl, 12 mM $NaHCO_3$, 20 mM HEPES, 5 mM glucose, 1 mM $MgCl_2$, and pH 7.3), platelets were resuspended in HEPES/Tyrode buffer for sample preparation.

Cell Fixation and Immunostaining

For the coating experiments, all steps were performed manually to evaluate the prerequisites for cell attachment and retention onto each substrate. The IF sample preparation protocol used was based on the protocol established for adherent cells by Stadler et al,[13] now being the standard protocol used to systematically explore subcellular protein localization in the HPA project at proteome wide scale. The conclusions from this study showed that fixation using 4% paraformaldehyde (PFA) and subsequent permeabilization with 0.1% Triton X-100, retained all cellular structures while giving access to epitopes in all membrane bound organelles and also subnuclear structures like nucleolus.

Shortly, cells were fixed with ice cold 4% PFA (43368.9M, VWR Stockholm, Sweden) for 15 min and permeabilized with 0.1% (w/v) Triton X-100 solution diluted in PBS for 3 times 5 min. Primary antibodies were diluted in blocking buffer (PBS with 4% FBS (F7524, Sigma-Aldrich) and cells were incubated overnight at 4C. Following four washing steps with 1x PBS, secondary antibodies were added at room temperature for 90 min, followed by incubation with the nuclear stain 4,'6-diamidino-2-phenylindole (DAPI) at 2.28 µM solution for 10 min at room temperature. Eventually cells were washed four times with 1x PBS cells were mounted in 85% glycerol before plates were sealed with aluminum foil covers.

For imaging of platelets, glass coverslips were coated with 50 µg/ml human fibrinogen in PBS for 1 hr prior to washing in PBS. Platelets (2×10^7/ml) were incubated on fibrinogen-coated cover glass (45 min, 37C) prior to fixation and staining as previously described.[15]

Antibodies

Primary rabbit polyclonal antibodies generated within the HPA project and distributed by Atlas Antibodies (Stockholm, Sweden) were diluted to 2 to 4 µg/ml. A mouse monoclonal anti-alpha tubulin antibody (Ab7291, Abcam, Sweden) diluted to 0.5 µg/ml) and a rat monoclonal anti-KDEL antibody (ab50601, Abcam

Sweden) diluted to 2.5 µg/ml were used as common markers for the cytoskeleton and endoplasmic reticulum (ER) respectively. Secondary antibodies goat anti-rabbit IgG Alexa-Fluor 488 (**A11034)**, goat anti-mouse IgG Alexa-Fluor 555 (**A21424**), and goat anti-rat IgG Alexa-Fluor 647 (**A21247**) (all from Thermo Fischer Scientific, Waltham, MA) were diluted to 2.5 µg/ml in blocking buffer.

Adherent platelets were stained with antisera against vinculin (Sigma, V9131), filamin A (Santa Cruz Biotechnology, Dallas, TX; sc-17749), non-muscle myosin IIa heavy chain (MYH9, Abcam, Cambridge, UK; ab89837), P-selectin (Santa Cruz Biotechnology; vsc-8419), and reticulon-4 (RTN4, Santa Cruz Biotechnology; sc-271878). Following staining with primary antibodies, platelets were stained with secondary antibodies and TRITC-phalloidin (Sigma, P1951).[15]

Automated Sample Preparation Protocol

The liquid handling robot Tecan Freedom EVO (Tecan Nordic Ab, Stockholm, Sweden) was used for automated plate preparations of cells and three new scripts were created and tested on the panel of different suspension cell lines. Each of the new scripts were optimized to change one off the following parameters during the sample preparation: (1) The number of washing steps after primary and secondary antibody staining were reduced from four to three, (2) the aspirated volume was decreased to always leave 10 µl of liquid remaining in the well, and (3) the pipetting speed was reduced from 4 to 0.5 µl/s. All liquid handling scripts used by the Tecan Freedom EVO can be found in the repository at Github (www.github.com; DOI 10.5281/zenodo.3463285).

Image Acquisition

For evaluation of cell distribution over entire wells, images were acquired automatically with the Leica inverted DMi8 widefield microscope (equipped with a HC PL FLUOTAR 4x/0.13 or 20x/0.4 N/A air objective and Hamamatsu Flash 4.0 V3 camera package) using the Leica Application Suite X (LAS X) software with the Leica LASX Navigator function. To allow for capturing of the entire well, several tiles were acquired and merged to generate the whole well image. The exposure time for all tiles from the same well was kept the same. For each tile the Leica Adaptive Focus Control (AFC) function was used to capture the best focus for each tile. The brightness in each tile can thus vary and separate tiles can be seen in some of the merged images. For wells acquired on separate days, exposure time and thus brightness can vary as no fixed settings for this image capturing was applied.

The Leica SP5 or SP8 confocal laser scanning microscope (CLSM), equipped with a 63x/1.4 N/A oil immersion objective, was used to acquire high-resolution images to allow for quality evaluation of fixation and organelle staining patterns. The images were acquired at room temperature in sequential steps using the following settings: 16-bit acquisition, pixel size 0.08 µm x 0.08 µm, line averaging of 2 and a pinhole of 1 airy unit (AU), scan speed 600 Hz (1.66 ms/pixel).

Image Analysis and Cell Counting

Images acquired from the DMi8 microscope for quantification and cell distribution purposes were processed using Fiji Is Just ImageJ (Fiji)[16] to enhance contrast of the cell nuclei for illustrative purposes. All images were also rescaled to 8 bit (dynamic range of 1–255) to reduce the file size. For high resolution images, brightness and contrast were automatically adjusted where needed for illustration purposes using Fiji. Cell Profiler[17] was used to quantify the number of cells in each well from the different experiments. For each cell line, 16 replicate samples (wells) were prepared (7 or 8 wells for REH due to insufficient number of cells for 16 wells). For every sample, image analysis was used to count cell nuclei and calculate the fraction of remaining cells compared to seeded cells. The Cell Profiler pipe line for cell quantification can be found in the repository at Github, DOI 10.5281/zenodo.3463285.

Results

Evaluation of Suspension Cell Adherence to a Variety of Coatings

As a first step in developing a high throughput protocol for IF of suspension cells, different coating materials were used to find the coating with the best prerequisites for retaining cells at a good density and even distribution across the sample well. To ensure as good image quality as possible, only glass bottom plates were used. These initial experiments focused on the human T-cell derived Jurkat cell line which represents a commonly used suspension cell line model in immunology and hematology studies. Replicate wells were coated with the different ECM proteins FN, LN, or Matrigel, containing a mixture of LN, collagen and entactin.[18] The synthetic polymers poly-L-ornithine and poly-L-lysine were also evaluated as they are popular coatings for plastic culture vessels and considerably cheaper than biological coatings.

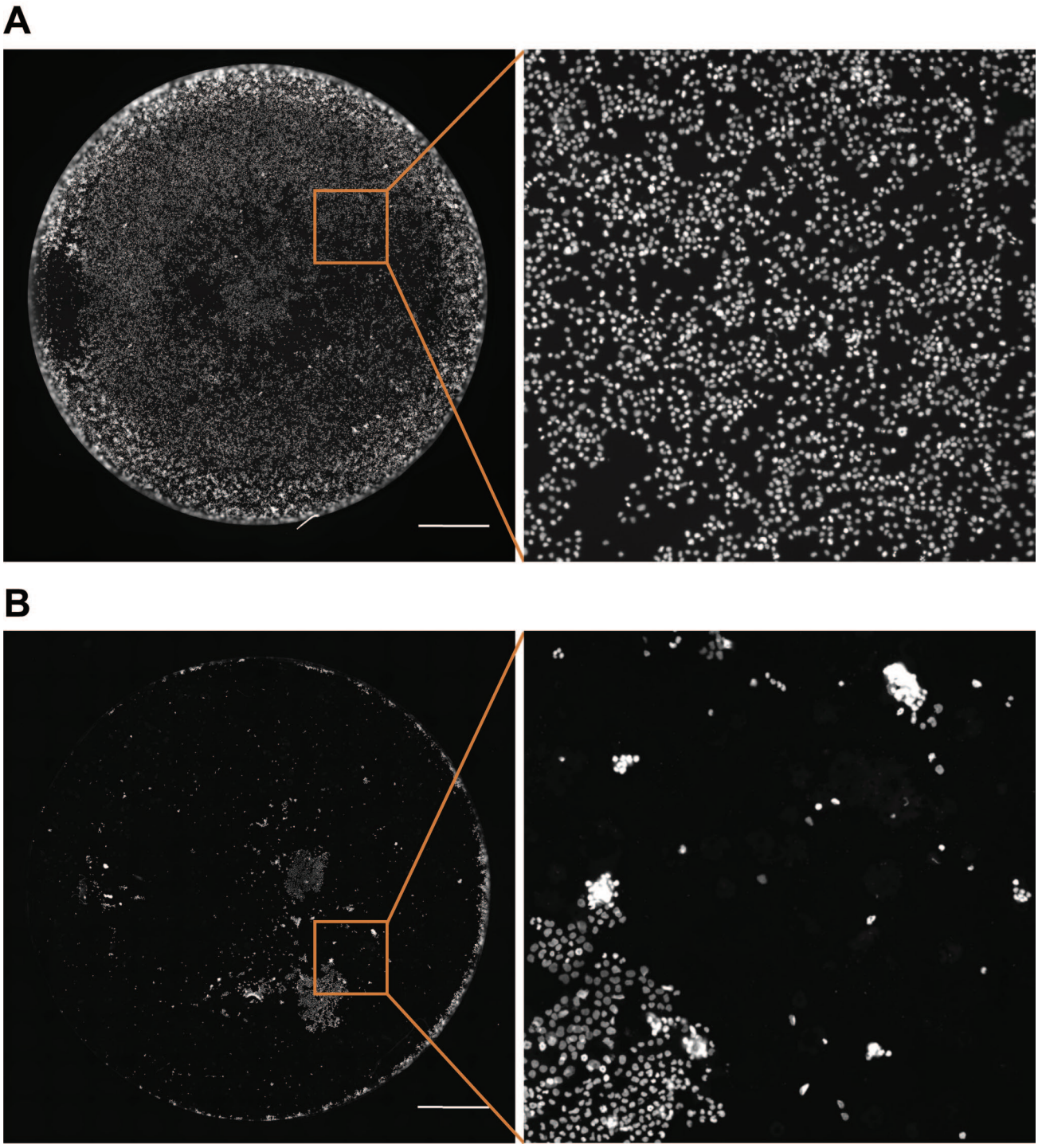

Figure 1. Representation of differences in cell density and distribution in two wells coated with fibronectin (A) and poly-L-lysine (B) from a 96-well plate. Cell nuclei are stained with DAPI and wells acquired with a 20x air objective. Scale bar is 1000 µm and cropped regions equal 1000 µm x 1000 µm. Abbreviation: DAPI, 4′,6-diamidino-2-phenylindole.

The highest number of remaining cells after the complete IF protocol was observed with FN. These samples show an even distribution of cells in the well in a reproducible manner (Fig. 1A). For all other coatings, an unevenly distributed cell population with considerably lower cell density was observed, even with high concentration of coating material. In many cases, only small clusters of cells or cells at the immediate edges

of the well were observed, as represented in Fig. 1B. For Matrigel, the results between the wells varied significantly, both between the two coating protocols used (incubation for a short time at room temperature vs long time at 4C) and for the replicate wells. The cells also clumped together on this surface resulting in a very uneven distribution of cells. The Matrigel protocol was also the most challenging coating protocol to use, requiring fast handling of the material with chilled pipette tips. Supplementary Fig. 1 show a subset of all wells acquired for each of the five different coatings and concentrations.

As we aimed to obtain a reproducible protocol suitable for high throughput sample preparation and imaging, we selected FN for coating throughout the rest of the study. The FN coating is also routinely used for seeding of adherent cells, giving reproducible results across multiple cell lines for hundreds of plates prepared over several years (data not shown). Since FN is a ubiquitously expressed constituent of the ECM,[19] we speculate other suspension cell lines to have good prerequisites for attaching to this coating as well.

Automated Sample Preparation of Suspension Cells Using Liquid Handling Robotics

Next, to standardize and ensure the reproducibility of high throughput sample preparation of suspension cells, we tested a previously developed automated liquid handling protocol with a Tecan Freedom EVO "robot," on five different suspension cell lines: HEL, THP1, REH, K-562, and Jurkat. To compare the fraction of remaining cells to a "best case scenario" the adherent cell line U-2 OS was used as a reference.

Figure 2A shows the distribution of cells in a representative well for each cell line. The images show that HEL, THP1, and U-2 OS to a large extent remain in the wells after completed sample preparation while most of K-562, Jurkat, and REH cells were detached using this protocol. Quantitative data from cell nuclei counting reveal that for both HEL and THP1 the number of detected cells exceeds that of the seeded cell number, showing that cells are not only remaining but also divide from time of seeding until fixation 24 hr after (Supplementary Fig. 2). Furthermore, the high number of cells and even distribution of HEL, THP1, and U-2 OS cells was observed for all wells analyzed, with a coefficient of variation (CV) of 7% for HEL, 19% for THP1, and 14% for U-2 OS. For K-562, Jurkat. and REH many cells were lost and only a small fraction of cells (19%, 17%, and 13% respectively) remained, mostly at the edges of the wells. The remaining cell number for these cell lines also varied more, with a CV of 46% for K-562, 23% for Jurkat, and 16% for REH. The CV for REH was better than for many cell lines, however as a consequence of having almost no cells left in any of the wells.

To improve the fraction of remaining K-562, Jurkat and REH cells the pipetting protocol for the liquid handling robot was optimized. While the conditions for fixation, permeabilization and immunostainings was identical to the original protocol, the number of washing steps or other instrument parameters were optimized. In total, three different protocols were tested differing from the standard protocol as follows: (1) The number of washing steps after primary and secondary antibody staining were reduced from four to three, (2) the aspirated volume was decreased to always leave some liquid in the wells, and (3) the pipetting speed was reduced from 4 to 0.5 µL/s. Sixteen samples of each cell line (8 for REH) were prepared, imaged, and evaluated by comparing remaining cells after completed sample preparation with the standard protocol and U-2 OS reference cell line. Figure 2B shows representative wells from the different pipetting protocols for Jurkat, K-562, and REH, and the average number of cells remaining from the different protocols (Fig. 2C). Based on this, the slow pipetting protocol resulted in the largest fraction of remaining cells for all cell lines. Compared to the standard protocol, the average fraction of remaining cells increased from 17% to 48% for Jurkat, 19% to 52% for K-562, from and 13% to 42% for REH. The CV was also calculated for the respective cell line and compared to the original standard protocol. For Jurkat the CV was the same, whereas it was reduced from 46% to 32% for K-562. While the overall number of remaining REH cells was greatly improved, the CV increased from 16% to 33%. These results suggest that lower pipetting speed gives better prerequisites for retaining a larger fraction of cells during the sample preparation. The quantitative data for each cell line and protocol are shown in Supplementary Fig. 3.

Compared to HEL and THP1, the Jurkat, K-562, and REH cells detached to a much higher extent also with the optimized protocol. To investigate this further, we looked at RNA expression data (normalized transcripts per million reads—tpm) generated within the HPA for 43-cell adhesion proteins in the integrin and cadherin families (Table 2). When comparing the sum of RNA transcript levels for these 43 genes, the lowest numbers were obtained for K-562 and REH (total tpm = 67 for both respective cell lines), while for HEL the number was equally high as for the adherent U2OS cell line (total tpm = 258 and 243, respectively). For THP1, the sum of RNA transcripts was also relatively high (total tpm = 195) while being lower for Jurkat (total tpm = 94). While expression level per gene is not very similar

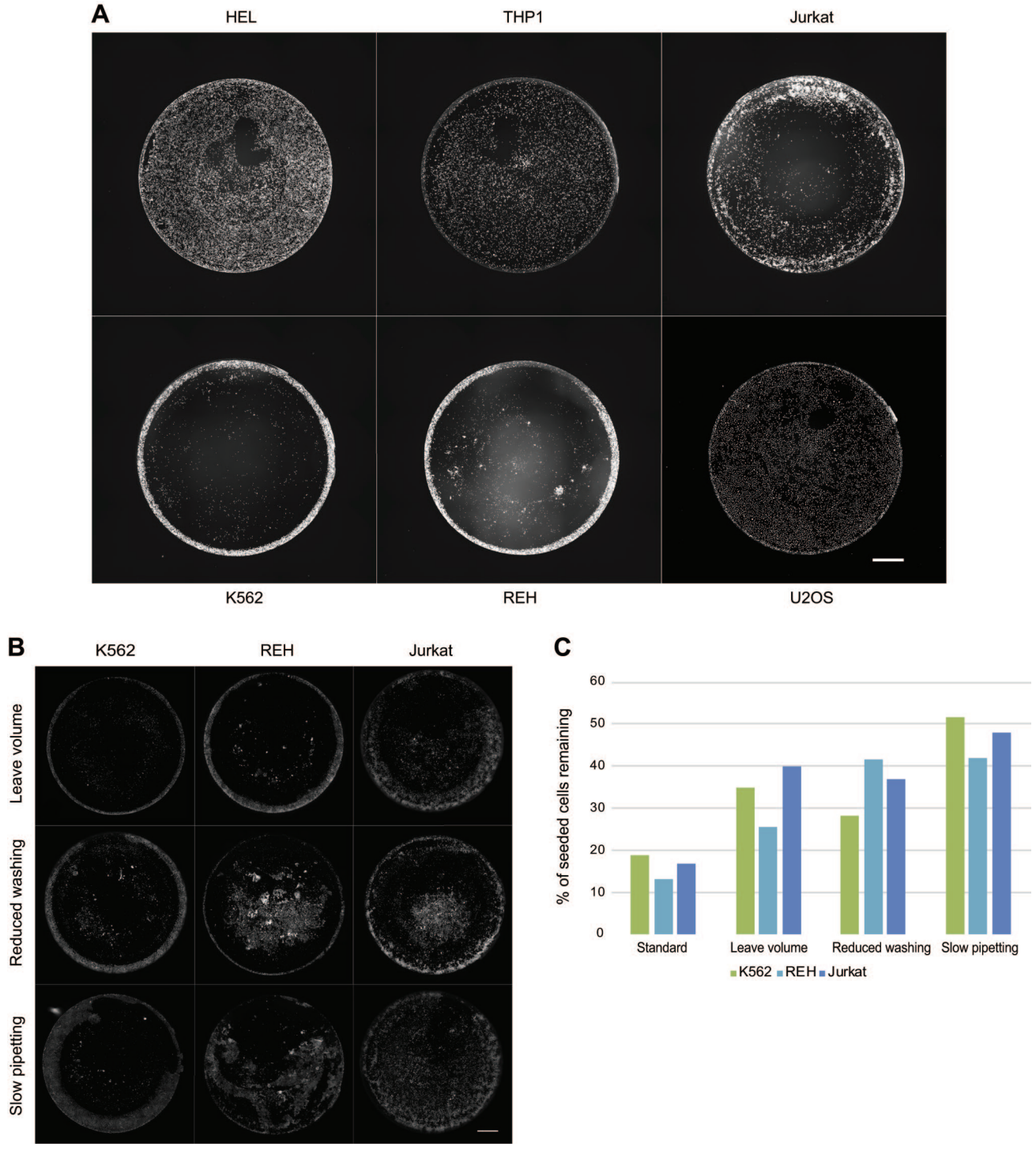

Figure 2. (A) Representative images showing cell distribution for each cell line using the automated protocol normally used for adherent cells. Images were acquired with a 20x air objective. *Upper row*: HEL, THP1 and Jurkat. *Lower row*: K-562, REH and U-2 OS. Scale bar: 1000 µm. (B) Representative images showing cell distribution for K-562 (left), REH (middle) and Jurkat (right) cell line using the three optimized protocols: leave volume (upper row), reduced washing steps (middle row) and slow pipetting (bottom row). (C) Bar chart showing the average fraction of remaining cells from replicate wells for K-562, REH, and Jurkat cells, for each of the three optimized automated protocols.

across cell lines, the summarized RNA transcript levels indicate a higher expression of adhesion proteins for HEL and THP1 compared to Jurkat, K-562, and REH. Further, HEL and THP1 have the highest number of

Table 2. RNA Sequencing Data for Adhesion Proteins Across the Cell Lines in the Study.

ENSG	Gene	Gene desc	HEL (norm. tpm)	JURKAT (norm. tpm)	K-562 (norm. tpm)	REH (norm. tpm)	THP-1 (norm. tpm)	U-2 OS (norm. tpm)
ENSG00000039068	CDH1	cadherin 1	0.02	0	0	0.02	0.07	0.17
ENSG00000040731	CDH10	cadherin 10	0	0	0	0	0	0.52
ENSG00000140937	CDH11	cadherin 11	0	0	0.01	0.17	0.03	3.56
ENSG00000154162	CDH12	cadherin 12	0.48	0.05	0.08	0.25	0.03	3.13
ENSG00000140945	CDH13	cadherin 13	0.09	0.07	0.09	0.03	0.09	5.11
ENSG00000129910	CDH15	cadherin 15	0.04	0.03	0.04	0.02	0	0.13
ENSG00000166589	CDH16	cadherin 16	0	0.01	0	0	0	0.03
ENSG00000079112	CDH17	cadherin 17	0.11	0.19	0.17	0.28	0.25	0.24
ENSG00000145526	CDH18	cadherin 18	0.3	0.12	0.24	0.02	0	9.18
ENSG00000071991	CDH19	cadherin 19	0.03	0.01	0.02	0.01	0.02	0.22
ENSG00000170558	CDH2	cadherin 2	0.01	2.56	0.01	0.03	0.09	11.59
ENSG00000101542	CDH20	cadherin 20	0.13	0	0.01	0	0	0
ENSG00000149654	CDH22	cadherin 22	0	0	0.02	0	0	0.17
ENSG00000107736	CDH23	cadherin related 23	1.26	0.55	0.13	1.47	2.83	1.48
ENSG00000139880	CDH24	cadherin 24	0.57	2.48	1.63	13	1.09	15.9
ENSG00000124215	CDH26	cadherin 26	5.36	0.43	0.07	0.01	0.42	0.04
ENSG00000062038	CDH3	cadherin 3	0	0.02	0	0.01	0.07	0.07
ENSG00000179242	CDH4	cadherin 4	0	0.31	0.02	0.04	0.06	14.57
ENSG00000179776	CDH5	cadherin 5	0.17	0	0.03	0.01	0.02	0.15
ENSG00000113361	CDH6	cadherin 6	0.03	0.01	0.02	0.01	0.06	0.42
ENSG00000081138	CDH7	cadherin 7	0.11	0.02	0.03	0.19	0.05	0.12
ENSG00000150394	CDH8	cadherin 8	0.1	0.01	0.37	0.01	0.02	0.65
ENSG00000113100	CDH9	cadherin 9	0.55	0.8	9.43	0.34	0.95	0.88
ENSG00000137809	ITGA11	integrin subunit alpha 11	0.14	0.03	0.05	0.05	0.16	0.3
ENSG00000005961	ITGA2B	integrin subunit alpha 2b	71.07	0.14	0.1	0.2	0.28	0.19
ENSG00000005884	ITGA3	integrin subunit alpha 3	0.02	1.06	0.02	0.05	0.28	20.42
ENSG00000115232	ITGA4	integrin subunit alpha 4	62.1	32.68	0.03	15.92	18.2	0.98
ENSG00000161638	ITGA5	integrin subunit alpha 5	2.93	1.59	2.5	1.41	8.22	6.76
ENSG00000091409	ITGA6	integrin subunit alpha 6	0.29	6.34	0.05	0.18	0.22	6.64
ENSG00000077943	ITGA8	integrin subunit alpha 8	2.39	0.02	0.04	0.05	0.05	0.05
ENSG00000005844	ITGAL	integrin subunit alpha L	0.46	1.48	0.02	0.05	4.39	0.02
ENSG00000169896	ITGAM	integrin subunit alpha M	0.67	0.01	1.15	0.2	2.77	0.07
ENSG00000138448	ITGAV	integrin subunit alpha V	2.24	1.16	2.19	0.02	4.32	12.62
ENSG00000140678	ITGAX	integrin subunit alpha X	0.07	0.02	0.08	0.09	1.51	0.78
ENSG00000150093	ITGB1	integrin subunit beta 1	14.81	6.13	10.22	3.78	11.99	54.75
ENSG00000119185	ITGB1BP1	integrin subunit beta 1 binding protein 1	16.46	13.84	9.19	12.83	9.61	17.97
ENSG00000160255	ITGB2	integrin subunit beta 2	2.41	8.12	0.11	0.25	117.56	1.07
ENSG00000259207	ITGB3	integrin subunit beta 3	41.28	0.66	0.14	0	0.06	0.71
ENSG00000142856	ITGB3BP	integrin subunit beta 3 binding protein	16.88	12.9	19.5	16.2	7.72	10.4
ENSG00000132470	ITGB4	integrin subunit beta 4	0.13	0.09	0.08	0.36	0.2	1.1
ENSG00000082781	ITGB5	integrin subunit beta 5	10.11	0.04	9.02	0.07	0.66	32.59
ENSG00000139626	ITGB7	integrin subunit beta 7	0.09	0.14	0.02	0.1	0.63	0.04
ENSG00000198542	ITGBL1	integrin subunit beta like 1	4.35	0	0.3	0.03	0.01	7.15
TOTAL			**258.26**	**94.12**	**67.23**	**67.76**	**194.99**	**242.94**

transcripts above 1 tpm, used as a cut-off to define expression of the corresponding protein in the HPA. As FN was used as coating material, the expression levels of the integrins ITGAV and ITGB1 should be the most important as these are the integrin subunits with specific affinity for FN.[15,17] Although the expression of these integrins is low in all cell lines as compared to U-2 OS, we speculate that the higher abundance of cell adhesion proteins overall in HEL and THP1 is favorable for improved attachment to any surface.

Manual and Automated Sample Preparation of Freshly Isolated PBMC and Platelets

To test the optimized slow pipetting protocol in primary cells, cells isolated from freshly withdrawn blood

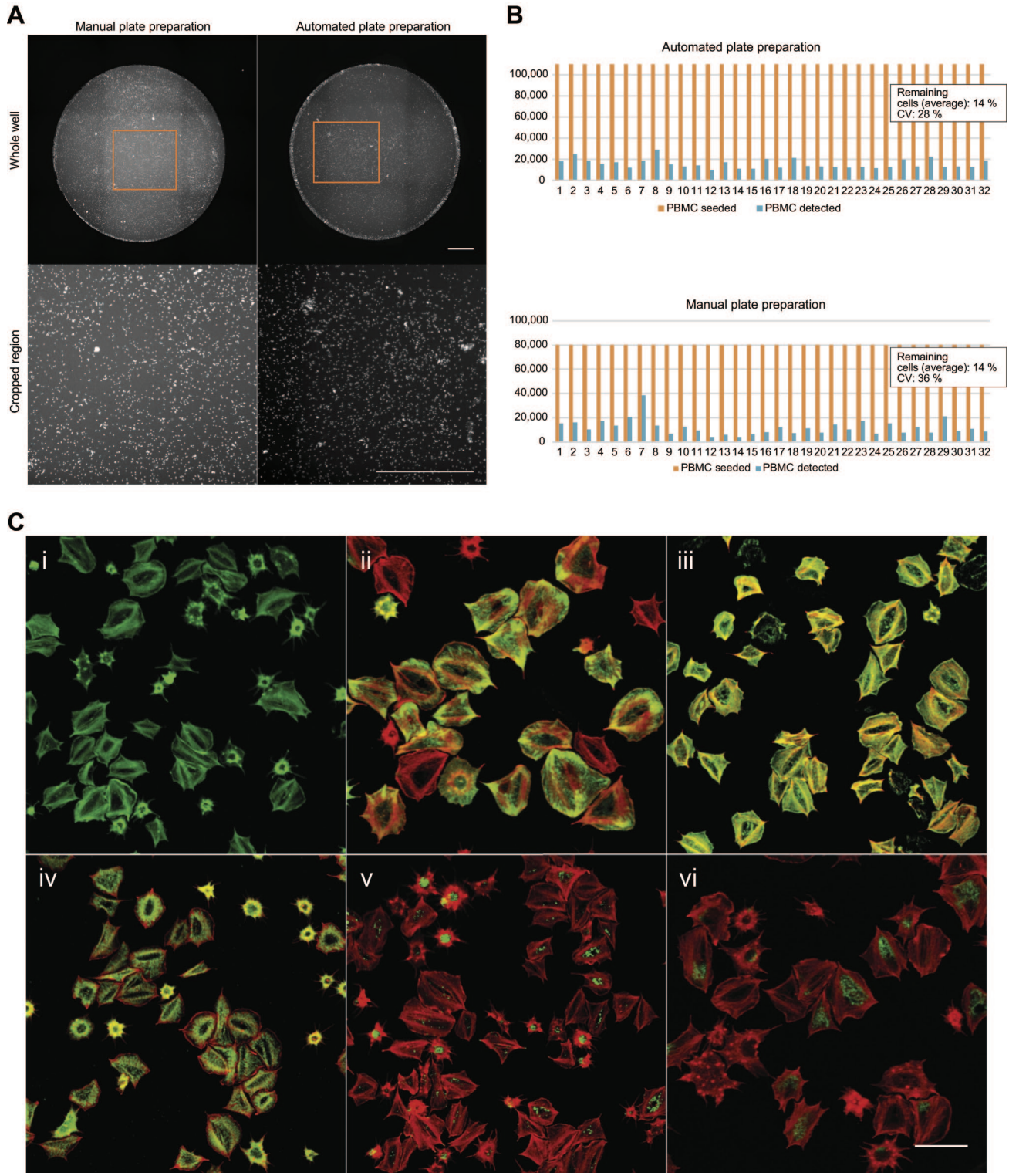

Figure 3. (A) Representative images of a whole well and corresponding cropped region from a manual versus automatic plate preparation. Scale bar:1000 µm. (B) Bar chart showing fraction of remaining PBMC in 32 individual wells from a manual versus automatic plate preparation. Total number of seeded cells for the automatically prepared plate is 110,000 and for the manually prepared plate 80,000. (C) Confocal images of selected structures in platelets. F-actin stained with phalloidin (i), actin filaments/focal adhesions stained for vinculin (ii), filamin A (iii) and myosin heavy chain 9 (iv), alpha granules stained for P selectin (v), and endoplasmic reticulum visualized by staining of RTN4 (vi). In panel ii-vi, the counter stain with phalloidin is shown in red. Images are acquired with a 63x oil immersion objective Scale bar: 10 µm.

(PBMC) were seeded and prepared either manually or using the optimized automated protocol with slow pipetting. Figure 3 shows a representative whole well image and cropped region of cell distribution from the respective preparations (Fig. 3A) and the number of remaining cells in 32 individual wells from manual and automatically prepared samples (Fig. 3B). The fraction of remaining cells is comparable for the manual and automated sample preparation, with 14% for both manually and automatically prepared wells and a CV of 36% and 28%, respectively (note that the number of seeded cells per well was 80,000 for the manually prepared plate and 110,000 for the automatically prepared plate). Even though this fraction is low, it shows that the automated protocol can be used as successfully as the manual one. Furthermore, the true fraction of remaining cells is likely higher than 14%, as platelets that are part of the PBMC sample when counting cells prior to seeding, cannot be detected as they lack a cell nucleus and thereby contains no DAPI stain.

To evaluate the quality and overall condition of blood cell preparations after fixation and sample processing, platelets were used as a representative peripheral blood cell for additional imaging analyses. Following fixation and permeabilization, washed human platelets adherent to fibrinogen were stained to visualize and evaluate their morphology (Fig. 3C). For all platelets, phalloidin was used to stain F-actin as a general marker for cell morphology. The phalloidin alone is shown in green in panel (i) and in red in for the following panels together with the respective protein targets; the cytoskeletal protein vinculin (VCL) (ii), the focal adhesion protein filamin A (FLNA) (iii), the non-muscle myosin IIa heavy chain (MYH9) (iv), the platelet alpha granule marker P-selectin (SELP, CD62P) (v), and RTN4 (vi), acting as a marker for ER of platelets.[20] Confocal microscopy at high resolution confirmed the presence of intact cytoskeletal filaments and intracellular structures representative of adherent platelets. The F-actin revealed platelets in different stages of adherence, being small and round at the beginning to gradually emerge into a more star shaped phenotype while actively spreading onto the surface. This morphological change mimics the normal process of adherence of platelets to endothelial cells and exposed ECM upon vascular injury.[21]

High Resolution Imaging of Organelle Markers in Suspension Cells

Finally, Jurkat cells were stained and imaged at high resolution to evaluate fixation quality and cell morphology. For this, cells were stained for the nucleus and the cytoskeleton using DAPI and an antibody targeting alpha tubulin for staining of the microtubules. Manual inspection of the cells showed a typical morphology for suspension cells with a relatively large nucleus and a small cytosol, shown in Fig. 4. To evaluate whether different subcellular structures could be distinguished within these suspension cells, marker proteins for eight major organelles were stained (Fig. 4A-H). For nuclear targets here represented by SRRM2 staining nuclear speckles (A) and DNAJB2 staining the nuclear membrane (B) the staining patterns are very similar to those of adherent cells and easily annotated. This is expected, as the cell nucleus itself is not that much smaller for suspension cells compared to adherent cells. Further, this structure is usually intact and the content well retained due to the nuclear membrane and anchoring to the ER. The Golgi apparatus here stained for GOLGA2 (C), is also easy to identify given it's dense structure and location in close proximity to the nucleus. Other cytosolic organelles such as vesicles (D—here represented by peroxisomes stained for AGP5) and mitochondria (E—here represented by staining of ETFA) were also reliably identified and can be distinguished between by the more regular and round shape of the vesicles compared to the mitochondria which are a bit more elongated and irregularly shaped. Staining of the ER stained for CALR (F) showed a netlike structure and the merge with the cell nucleus show co-localization at the nuclear membrane, often observed for staining of proteins in the ER. Staining of the plasma membrane here represented by staining of PEBP1 (G) looks very similar to a cytosolic stain. This distinction can be a challenge also when staining adherent cells. Looking at the merge with the microtubules, the PEBP1 stain spreads further from the cell nucleus compared to the microtubules, indicating staining of the plasma membrane in this case. Finally, the cytoskeletal structures as represented by the microtubules in all stainings and here by the intermediate filaments (H) stained for PGM2, could also be identified. These results suggest that the optimized protocol in combination with confocal microscopy is suitable for automated sample preparation for subcellular profiling of major organelles in suspension cells.

Discussion

In this work, we optimized a protocol for sample preparation for IF of suspension cells, compatible with cell lines as well as primary PBMC and platelet cells. In addition, this protocol was automated using liquid handling robotics to allow for high-throughput applications.

By optimizing different parameters, the fraction of remaining cells could be increased for all tested cell

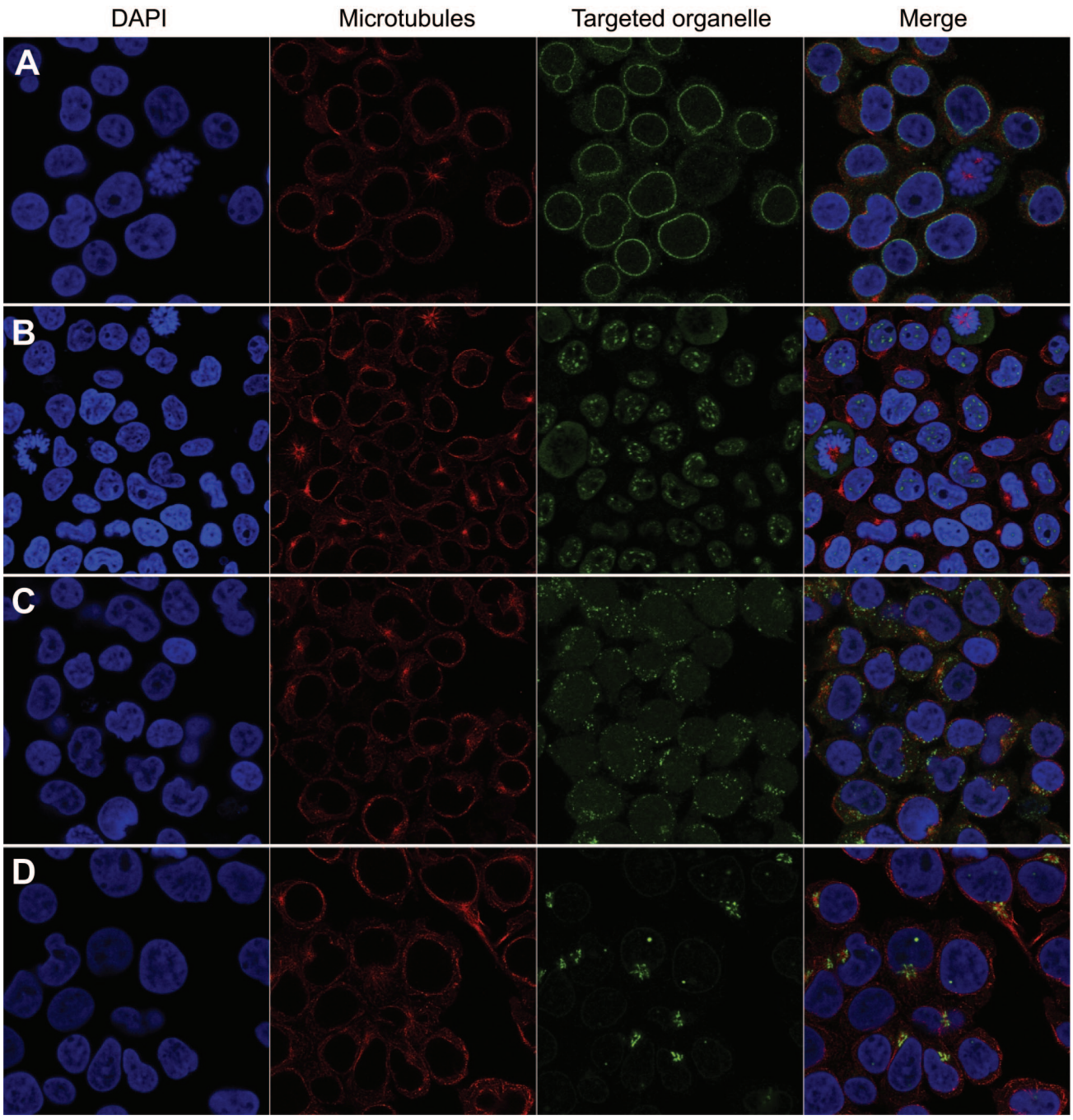

(continued)

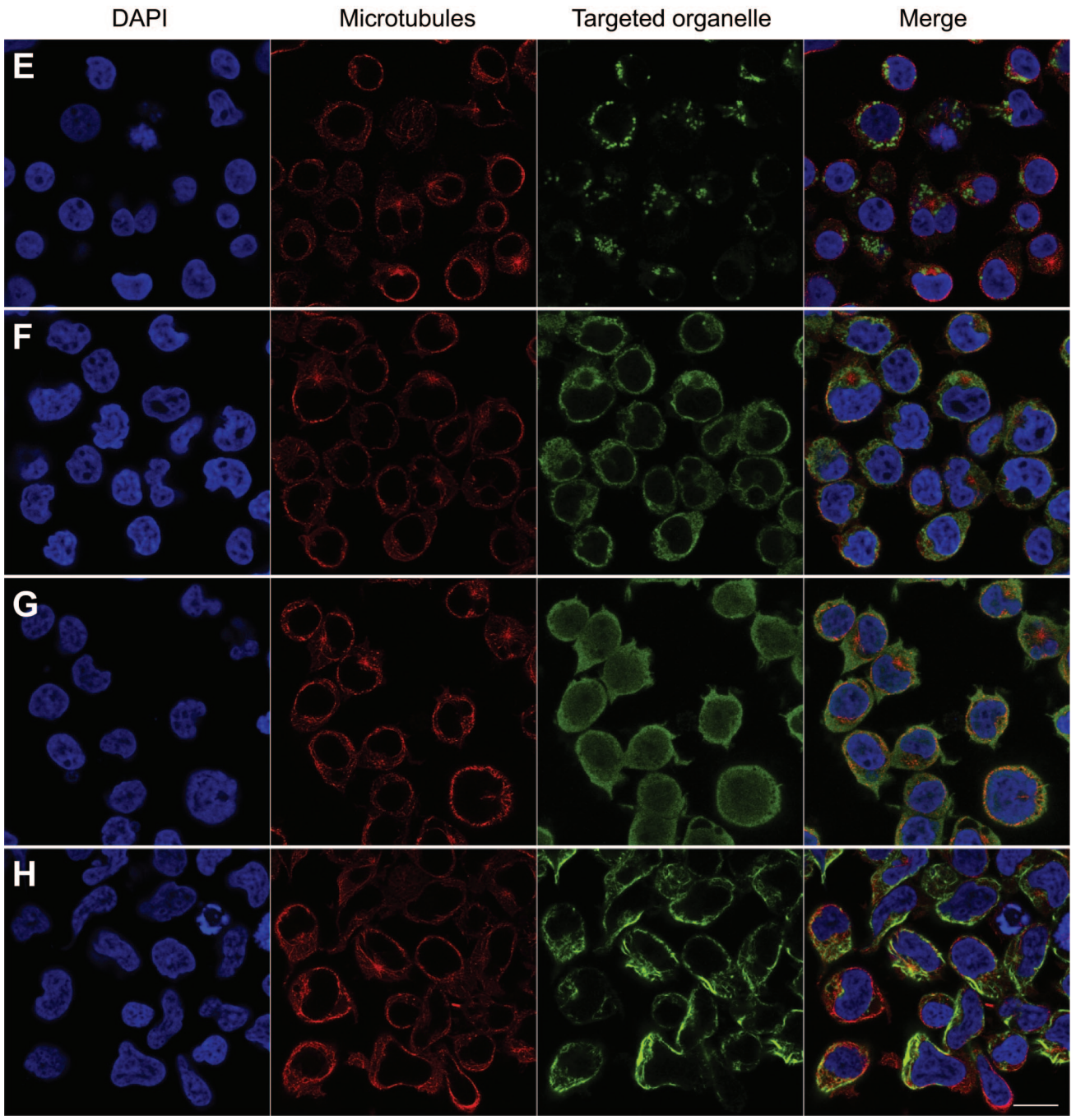

Figure 4. Confocal images of Jurkat cells, stained for DAPI (first column), microtubules (second column) and the respective targeted organelle (third column): nuclear speckles (A), nuclear membrane (B), Golgi apparatus (C), peroxisomes (D), mitochondria (E), endoplasmic reticulum (F), plasma membrane (G), and intermediate filaments (H). A merge of the common markers and the organelle is shown in the right column. Images are acquired with a 63x oil immersion objective. Scale bar: 10 μm. Abbreviation: DAPI, 4′,6-diamidino-2-phenylindole.

lines, with the best results obtained by reducing the pipetting speed to minimal. This parameter is in our experience is the most critical for a successful manual sample preparation of any cell line, as it reduces the shear forces on the cells. Given that all individual parameters (reduced aspiration volume, reduced number of washing steps, and reduced pipetting speed) resulted in a larger fraction of remaining cells, it is likely that a protocol combing all of these parameters would generate even better results in terms of

remaining cells. However, the reduced number of washing steps is not ideal since it might affect background and thus overall quality of the images. In case of the parameter of a lower volume being aspirated throughout the protocol, this slightly changes the concentration and exposure time of reagents and should therefore be evaluated more carefully before being implemented. Still, this is something to consider for further improvements. In this study, different fixation protocols were not tested as this has been evaluated in previous studies by Stadler et al.[13] However, certain target proteins are better detected using other fixatives like methanol. Using such protocol when relevant could potentially have a positive impact on the number of remaining cells as fixation and permeabilization is obtained within the same step and reduces the total number of washing steps.

We observed different overall success in remaining cell number and CV for the different cell lines used in this study. Our evaluation of cell adhesion protein expression by RNA sequencing data, indicates higher overall expression of adhesion proteins in HEL and THP1, lower for Jurkat and lowest for K-562 and REH. This correlates well with the number of remaining cells and also with the robustness, as HEL and THP1 where the cell lines with highest fraction of reaming cells and smallest CV. Based on this, the RNA expression data available in the HPA database for a broad panel of cell lines, could be a useful tool when selecting cell lines for imaging, or in selecting the most suitable coating for a particular cell line, depending on the expression of specific integrins. Besides expression of cell adhesion proteins, the size of cells could be relevant for how well they attach. For example, the HEL and THP1 cell lines are considerably larger than K-562 and REH, suggesting more binding events to the surface and thus a stronger attachment. In our experience, smaller cells like K-562 and REH aggregate more easily and are harder to homogenize in the solution prior to seeding. We believe this can have an impact of the overall CV of remaining cells as cell number within wells are more likely to differ than those of larger cells. To get a more precise fraction of remaining cells in each well, cells would have to be counted before starting the sample preparation. In this work however, the primary aim was to increase the number of remaining cells by optimizing sample preparation, excluding cell seeding conditions.

There are two important aspects improved by this protocol compared to imaging of cells on glass slides. First, the plate format allows for much higher throughput compared to staining of cells on cover glasses. Second, the sample prep to more easily automated using liquid handling robots, making the sample preparation more robust. This is required for systematic studies with hundreds of proteins being imaged. In addition to establish an automated protocol for sample preparation allowing for high throughput, we also demonstrate how IF can successfully be used for protein localization at subcellular level in suspension cell lines as well as in platelets. This enables systematic exploration of the intracellular landscape of different cell types derived from blood, and provide an important complement to flow-based methods lacking the spatial information obtained from imaging. The developed protocol also serves complementary to other imaging methods for cells in suspension, such as imaging flow cytometry,[22] by allowing high-resolution imaging and analysis of cell–cell interactions.

Recently generated data within the framework of the HPA using Mass Cytometry (CyTOF) and RNA sequencing of 18 specific cell types from PBMC, suggest almost 1500 protein coding genes to have an elevated expression in any of the six hematopoietic cell lineages (T-cells, B-cells, NK cells, monocytes, granulocytes, and dendritic cells).[23] This makes it highly relevant to better explore their intracellular proteomes. The data above are part of the HPA effort in creating a Blood Atlas, which was recently released as a complement to the three existing sub atlases: Tissue Atlas, Cell Atlas, and the Pathology Atlas.

The optimized protocol from this work allows for high throughput sample preparation and imaging of suspension cells, that in combination with the proteome wide collection of antibodies generated within the HPA project presents, opportunities to create a subcellular map of immune cells as a way to better understand the immune system in health and disease.

Acknowledgments

We acknowledge Knut and Alice Wallenberg foundation (KAW) for their generous support to the Human Protein Atlas project, which instrumentation has been used to conduct this work and Science for life laboratories for funding the Cell Profiling Facility at Royal Institute of Technology that has been instrumental for the entire work from cell cultivation to sample preparation and microscopy.

Competing Interests

The author(s) declared no potential conflicts of interest with respect to the research, authorship, and/or publication of this article.

Author Contributions

AB, LK, and CG performed the cell cultivations, coatings, and stainings of cell lines. AB and LK isolated and prepared the PBMC. CG optimized the pipetting protocols on the Tecan Freedom EVO Robot. AB, LK, HX, and CS did the image acquisition. AB and CS performed the quantitative

image analysis. JA isolated and stained the platelets, provided intellectual input and contributed to the manuscript. EL provided intellectual input and contributed to the manuscript. CS wrote the manuscript, made all figures, designed, and led the study. Each author has read and approved the manuscript prior to submission.

Funding

The author(s) disclosed receipt of the following financial support for the research, authorship, and/or publication of this article: This work has been done within the Cell Profiling Facility at the Royal Institute of Technology, funded by Science for Life Laboratory, the National Microscopy Infrastructure, NMI (VR-RFI 2016-00968) and supported by the EPIC-XS consortium, project number 823839, funded by the Horizon 2020 program of the European Union.

Literature Cited

1. Thul PJ, Akesson L, Wiking M, Mahdessian D, Geladaki A, Ait Blal H, Alm T, Asplund A, Bjork L, Breckels LM, Backstrom A, Danielsson F, Fagerberg L, Fall J, Gatto L, Gnann C, Hober S, Hjelmare M, Johansson F, Lee S, Lindskog C, Mulder J, Mulvey CM, Nilsson P, Oksvold P, Rockberg J, Schutten R, Schwenk JM, Sivertsson A, Sjostedt E, Skogs M, Stadler C, Sullivan DP, Tegel H, Winsnes C, Zhang C, Zwahlen M, Mardinoglu A, Ponten F, von Feilitzen K, Lilley KS, Uhlen M, Lundberg E. A subcellular map of the human proteome. Science. 2017;356(6340):eaal3321. doi:10.1126/science.aal3321.
2. Uhlen M, Fagerberg L, Hallstrom BM, Lindskog C, Oksvold P, Mardinoglu A, Sivertsson A, Kampf C, Sjostedt E, Asplund A, Olsson I, Edlund K, Lundberg E, Navani S, Szigyarto CA, Odeberg J, Djureinovic D, Takanen JO, Hober S, Alm T, Edqvist PH, Berling H, Tegel H, Mulder J, Rockberg J, Nilsson P, Schwenk JM, Hamsten M, von Feilitzen K, Forsberg M, Persson L, Johansson F, Zwahlen M, von Heijne G, Nielsen J, Ponten F. Proteomics. Tissue-based map of the human proteome. Science. 2015;347(6220):1260419. doi:10.1126/science.1260419.
3. Uhlen M, Oksvold P, Fagerberg L, Lundberg E, Jonasson K, Forsberg M, Zwahlen M, Kampf C, Wester K, Hober S, Wernerus H, Bjorling L, Ponten F. Towards a knowledge-based Human Protein Atlas. Nat Biotechnol. 2010;28(12):1248–50. doi:10.1038/nbt1210-1248.
4. Lundberg E, Fagerberg L, Klevebring D, Matic I, Geiger T, Cox J, Algenas C, Lundeberg J, Mann M, Uhlen M. Defining the transcriptome and proteome in three functionally different human cell lines. Mol Syst Biol. 2010;6:450. doi:10.1038/msb.2010.106.
5. Nagaraj N, Wisniewski JR, Geiger T, Cox J, Kircher M, Kelso J, Paabo S, Mann M. Deep proteome and transcriptome mapping of a human cancer cell line. Mol Syst Biol. 2011;7:548. doi:10.1038/msb.2011.81.
6. Stadler C, Fagerberg L, Sivertsson A, Oksvold P, Zwahlen M, Hallstrom BM, Lundberg E, Uhlen M. RNA- and antibody-based profiling of the human proteome with focus on chromosome 19. J Proteome Res. 2014;13(4):2019–27. doi:10.1021/pr401156g.
7. Danielsson F, Wiking M, Mahdessian D, Skogs M, Ait Blal H, Hjelmare M, Stadler C, Uhlen M, Lundberg E. RNA deep sequencing as a tool for selection of cell lines for systematic subcellular localization of all human proteins. J Proteome Res. 2013;12(1):299–307. doi:10.1021/pr3009308.
8. Liberio MS, Sadowski MC, Soekmadji C, Davis RA, Nelson CC. Differential effects of tissue culture coating substrates on prostate cancer cell adherence, morphology and behavior. PLoS ONE. 2014;9(11):e112122. doi:10.1371/journal.pone.0112122.
9. Attachment and matrix factors. BioFiles [Internet]. 2008;3(8) [cited 2018 Jan 13]. Available from: https://www.sigmaaldrich.com/content/dam/sigma-aldrich/flashapps/biofiles-movie/pdf/biofiles_issue3.8.pdf
10. Way L, Scutt N, Scutt A. Cytocentrifugation: a convenient and efficient method for seeding tendon-derived cells into monolayer cultures or 3-D tissue engineering scaffolds. Cytotechnology. 2011;63(6):567–579. doi:10.1007/s10616-011-9391-4.
11. Curiox. Available from: https://www.curiox.com/da-cell-plate-washing-station/
12. Harlow E, Lane D. Fixing suspension cells with paraformaldehyde. CSH Protoc. 2006;2006(3):pdb.prot4295. doi:10.1101/pdb.prot4295.
13. Stadler C, Skogs M, Brismar H, Uhlen M, Lundberg E. A single fixation protocol for proteome-wide immunofluorescence localization studies. J Proteomics. 2010;73(6):1067–78. doi:10.1016/j.jprot.2009.10.012.
14. Aslan JE, Itakura A, Gertz JM, McCarty OJ. Platelet shape change and spreading. Methods Mol Biol. 2012;788:91–100. doi:10.1007/978-1-61779-307-3_7.
15. Ngo AT, Thierheimer ML, Babur O, Rocheleau AD, Huang T, Pang J, Rigg RA, Mitrugno A, Theodorescu D, Burchard J, Nan X, Demir E, McCarty OJ, Aslan JE. Assessment of roles for the Rho-specific guanine nucleotide dissociation inhibitor Ly-GDI in platelet function: a spatial systems approach. Am J Physiol Cell Physiol. 2017;312(4):C527–36. doi:10.1152/ajpcell.00274.2016.
16. Schneider CA, Rasband WS, Eliceiri KW. NIH Image to ImageJ: 25 years of image analysis. Nat Methods. 2012;9(7):671–5.
17. Carpenter AE, Jones TR, Lamprecht MR, Clarke C, Kang IH, Friman O, Guertin DA, Chang JH, Lindquist RA, Moffat J, Golland P, Sabatini DM. CellProfiler: image analysis software for identifying and quantifying cell phenotypes. Genome Biol. 2006;7(10):R100. doi:10.1186/gb-2006-7-10-r100.
18. Hughes CS, Postovit LM, Lajoie GA. Matrigel: a complex protein mixture required for optimal growth of cell culture. Proteomics. 2010;10(9):1886–90. doi:10.1002/pmic.200900758.
19. Kleinman HK, Cannon FB, Laurie GW, Hassell JR, Aumailley M, Terranova VP, Martin GR, DuBois-Dalcq

M. Biological activities of laminin. J Cell Biochem. 1985;27(4):317–25. doi:10.1002/jcb.240270402.
20. Babur O, Ngo ATP, Rigg RA, Pang J, Rub ZT, Buchanan AE, Mitrugno A, David LL, McCarty OJT, Demir E, Aslan JE. Platelet procoagulant phenotype is modulated by a p38-MK2 axis that regulates RTN4/Nogo proximal to the endoplasmic reticulum: utility of pathway analysis. Am J Physiol Cell Physiol. 2018;314(5):C603–15. doi:10.1152/ajpcell.00177.2017.
21. Ruggeri ZM, Mendolicchio GL. Adhesion mechanisms in platelet function. Circ Res. 2007;100(12):1673–85. doi:10.1161/01.RES.0000267878.97021.ab.
22. Han Y, Gu Y, Zhang AC, Lo YH. Review: imaging technologies for flow cytometry. Lab Chip. 2016;16(24):4639–47. doi:10.1039/c6lc01063f.
23. Uhlen M, Karlsson MJ, Zhong W, Tebani A, Pou C, Mikes J, Lakshmikanth T, Forsstrom B, Edfors F, Odeberg J, Mardinoglu A, Zhang C, von Feilitzen K, Mulder J, Sjostedt E, Hober A, Oksvold P, Zwahlen M, Ponten F, Lindskog C, Sivertsson A, Fagerberg L, Brodin P. A genome-wide transcriptomic analysis of protein-coding genes in human blood cells. Science. 2019;366(6472):eaax9198. doi:10.1126/science.aax9198.

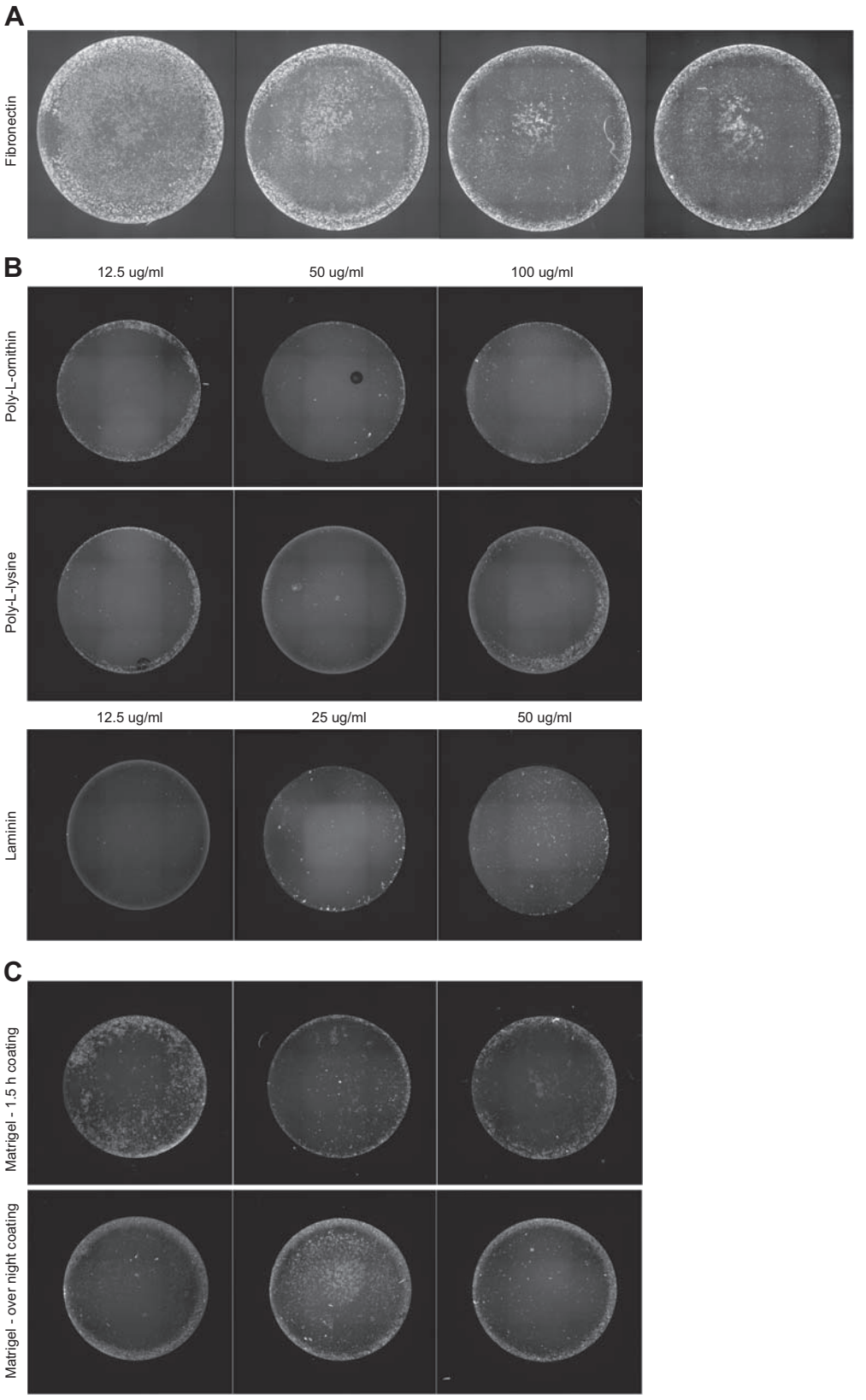

Supplementary Figure 1. Images showing distribution of Jurkat cells in wells coated with five different coatings at various concentrations.
A. Four replicate wells coated with 12.5 μg/ml fibronectin.
B. Representative wells coated with Poly-l-ornithin, poly-l-lysine and laminin with a concentration of 12.5 25, 50 or 100 μg/ml.
C. Representative wells coated with Matrigel diluted 1:30 and incubated 1.5 h at RT or overnight at 4 °C.

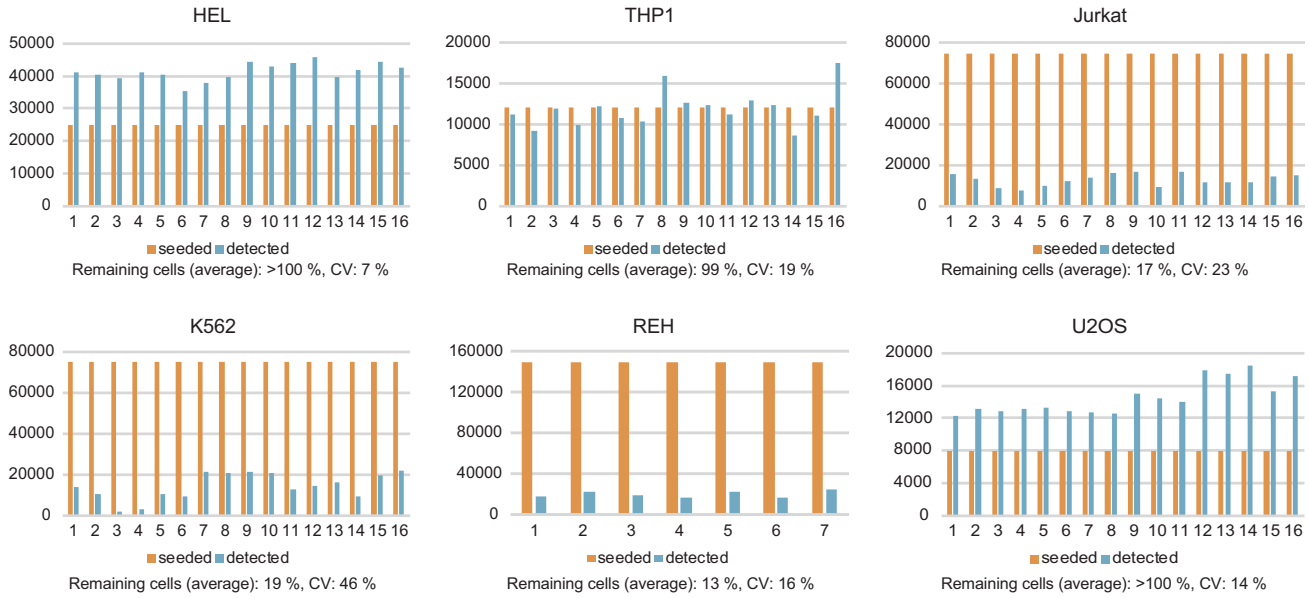

Supplementary Figure 2. Bar charts for each of the six cell lines showing the number of seeded (orange) and remaining (blue) cells (vertical axis) using the automated standard protocol. Each chart display values for 16 or 7 replicate wells (horizontal axis) along with a calculated CV and average number of remaining cells.

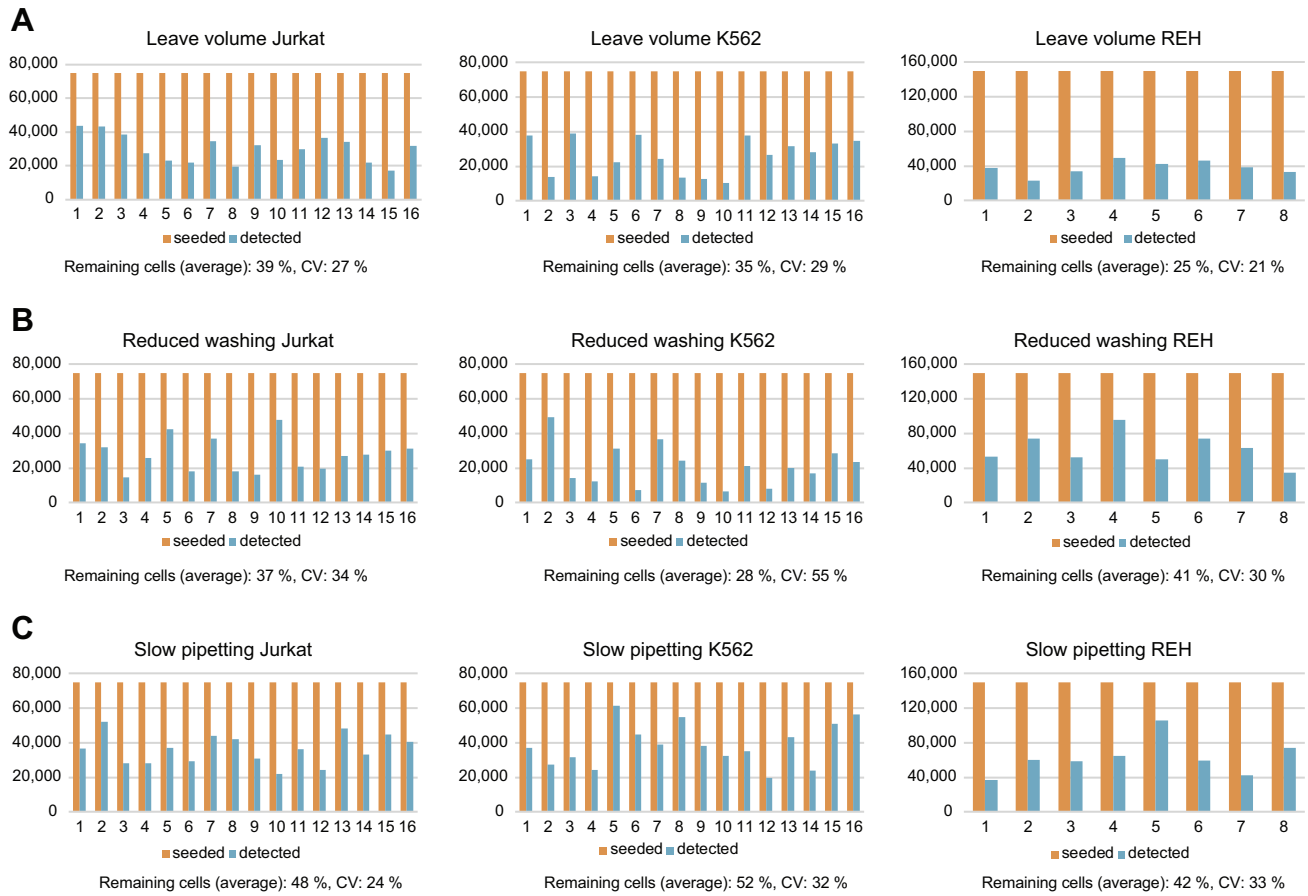

Supplementary Figure 3. Bar charts for Jurkat, K-562 and REH cell lines showing the number of seeded (orange) and remaining (blue) cells (vertical axis) using the **A.** leave volume protocol **B.** Reduced washing protocol and **C.** Slow pipetting protocol. Each chart display values for 16 or 8 replicate wells (horizontal axis) along with a calculated CV and average number of remaining cells.